Correlation of neoclassical and turbulent momentum fluxes mediated by poloidal convective cells

Xavier Garbet, P Asahi, P Donnel, P Ehrlacher, Guilhem Dif-Pradalier, Philippe Ghendrih, Virginie Grandgirard, Yanick Sarazin

Correlation of neoclassical and turbulent momentum fluxes mediated by poloidal convective cells

X. Garbet, Y. Asahi, P. Donnel, C. Ehrlacher, G. Dif-Pradalier, P. Ghendrih,V. Grandgirard, Y. Sarazin
CEA, IRFM, F-13108 St.Paul-lez-Durance cedex, France

Abstract

Radial fluxes of parallel momentum due to $E \times B$ and curvature (and ∇B) drifts are shown to be correlated in tokamak plasmas. This correlation comes from the onset of poloidal convective cells generated by turbulence. The entire process requires a symmetry breaking mechanism, e.g. a mean shear flow. An analytical calculation shows that anti-correlation between the poloidal and parallel components of the turbulent Reynolds stress results in anti-correlation of the fluxes of parallel momentum generated by $E \times B$ and curvature drifts.

1 Introduction

Interplay between neoclassical and turbulent transport processes has been recently uncovered thanks to the implementation of accurate collision operators in gyrokinetic codes. Examples of non trivial interaction have been found for heat [1, 2], momentum [3, 4, 5, 6, 7, 14] and particle [15] transport channels. Two types of mechanisms that may explain such an interplay have been proposed so far: turbulent collisional scattering in the velocity space, and interaction via large scale flows. This question is not always easy to apprehend in the literature, because of some differences in terminology and definitions. Turbulent transport is often defined as due to $E \times B$ drift contribution, while "neoclassical" is associated with curvature (and ∇B) drift. Though legitimate when looking at each problem separately, this definition is somewhat restrictive in the general case, since poloidal asymmetries of the $E \times B$ drift velocity may contribute to neoclassical transport [1]. It is therefore safer to talk about fluxes due to $E \times B$ and curvature drifts, while keeping in mind that they are somewhat representative of "turbulent " and "neoclassical" contributions.

Curvature and $E \times B$ drift components of fluxes were found anti-correlated in several global simulations of turbulent transport, when calculated on an equal footing. This is particularly striking for momentum transport [6, 7], and transport of impurities [15]. A hint of a similar behavior is observed in simulations of ion heat transport near

threshold [1]. A mechanism is proposed here to explain a correlation between the contributions of curvature and $E \times B$ drifts to momentum transport, based on turbulent generation of poloidal convective cells. The chain of causes starts with the well established correlation between $E \times B$ radial fluxes of parallel and poloidal momentum due to mean shear flow or any other mechanism responsible for an up-down asymmetry of turbulence intensity. Turbulence is ballooned in a tokamak, i.e. is more intense on the low field side. The resulting asymmetry of the turbulent stress tensor generates poloidal convective cells, i.e. flows that are zonal in the toroidal rotation, but not in the poloidal direction. It appears that these flows are weakly damped at low frequency, and drive poloidal asymmetries of the distribution function, which contribute to a non zero flux of parallel momentum due to curvature drift. Hence it appears that the curvature driven component of the flux of parallel momentum is tied to the $E \times B$ radial flux of poloidal momentum. Anti-correlation of the poloidal and parallel components of the turbulent Reynolds stress leads to anti-correlated radial fluxes of parallel momentum due to curvature and $E \times B$ drifts. This scheme is illustrated in Fig.1. A schematic view of the circulation pattern in a tokamak poloidal plane is also shown in Fig.2.

A simplified calculation is presented here, where the mean parallel velocity and its gradient are small. In other words only the residual stress tensor is calculated. It appears that the sign of the correlation between the poloidal and parallel components of the $E \times B$ Reynolds stress translates in a correlation of the curvature and $E \times B$ drift contributions to the radial flux of parallel momentum. This general result comes from a simple relationship between the momentum flux due to curvature and the turbulent Reynolds stress (summarized in Fig.2). Although poloidal convective cells do not appear explicitly in this relationship, they are instrumental to this mechanism. The overall process is illustrated by a quasi-linear calculation of stress tensors and fluxes based on linear Ion Temperature Gradient (ITG) driven modes in the hydrodynamic limit. This calculation predicts similar amplitudes for the ExB and curvature drift components of the parallel momentum flux, but a sign of correlation that depends on plasma parameters. Typically for modes drifting in the ion diamagnetic direction, positive correlation is found for weak drive, and anti-correlation for strong drive. Since the hydrodynamic limit is valid only in the strong drive limit, this result can be considered as encouraging in view of previous numerical calculations, which found anti-correlation [6, 7]. The fact that poloidal asymmetries of the turbulent generated flows produce a significant flux of momentum implies that neoclassical and turbulent

fluxes of momentum should be calculated all together.

The paper is organized as follows. General expressions of radial fluxes of parallel momentum are derived in section 2. The contribution from the curvature drift is detailed in section 3. The $E \times B$ and curvature driven fluxes of parallel momentum are compared and discussed in section 4. A conclusion follows.

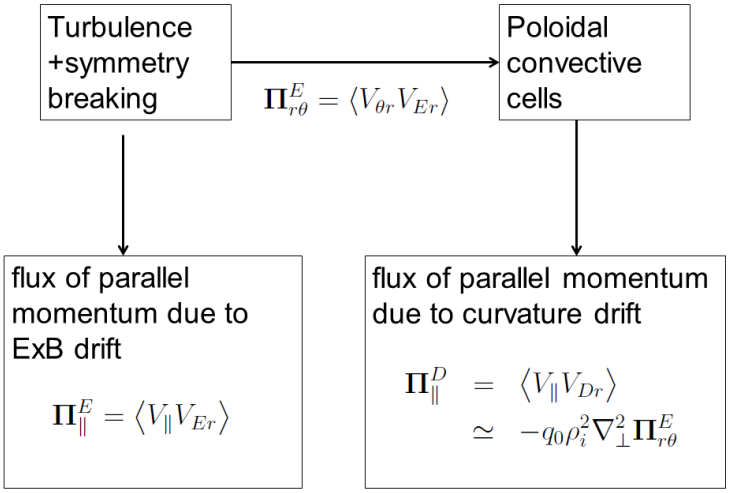

Figure 1: Schematic chart that illustrates the link between correlated radial fluxes of parallel momentum due to $E \times B$ and curvature drifts, and the correlation between the poloidal and parallel components of the turbulence stress tensor.

2 Fluxes of parallel momentum

Momentum flux is the same as the Reynolds stress tensor up to a mass density Nm, where N is the unperturbed density and m the ion mass. Both names will be used indistinctly throughout the paper. We calculate separately the contributions from the $E \times B$ drift and curvature drift velocities to the Reynolds stress tensor, i.e.

$$\mathbf{\Pi}^E_{\parallel} = \frac{1}{N} \int d^3\mathbf{v} F v_{\parallel} \mathbf{v}_E \tag{1}$$

and

$$\mathbf{\Pi}^D_{\parallel} = \frac{1}{N} \int d^3\mathbf{v} F v_{\parallel} \mathbf{v}_D \tag{2}$$

where F is the distribution function, $v_{\parallel}$ is velocity that is aligned with the unperturbed magnetic field, $\mathbf{v}_E$ is the $E \times B$ drift velocity and $\mathbf{v}_D$

is the drift velocity due to curvature and gradient of the unperturbed magnetic field. It is dubbed "curvature drift velocity" hereafter. The analysis is restricted to electrostatic turbulence, i.e.

$$\mathbf{v}_E = \mathbf{b} \times \frac{\nabla \phi}{B} \tag{3}$$

where ϕ is the electric potential, $\mathbf{b} = \frac{\mathbf{B}}{B}$ and $\mathbf{B}$ is the (unperturbed) magnetic field. Also we use a simplified expression of the curvature drift velocity, valid at low values of the plasma β and normalized gyroradius ρ_*,

$$\mathbf{v}_D = \frac{m}{eB}\left(\frac{v_\perp^2}{2} + v_\parallel^2\right)\mathbf{b} \times \frac{\nabla B}{B} \tag{4}$$

where m is the mass, e the charge, and $v_\perp$ is the modulus of the perpendicular velocity.

A simplified geometry of circular concentric magnetic surfaces is considered here. The spatial coordinates are (r, θ, φ), where r is the minor radius, θ and φ the poloidal and toroidal angles (see Fig.2). The corresponding unperturbed magnetic field is

$$\mathbf{B} = B_0 R_0 \left(\nabla\varphi + \frac{r}{q(r)R_0}\nabla\varphi \times \nabla r\right) \tag{5}$$

where R_0 the major radius, $q(r)$ the safety factor, and B_0 the magnetic field on the magnetic axis.

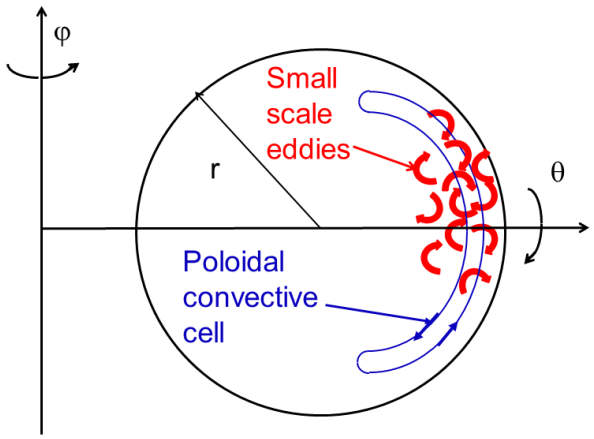

Figure 2: Schematic illustration of the flow pattern in a tokamak poloidal plane.

2.1 Turbulence parametrization

2.1.1 Electric potential fluctuations

Since an evaluation of the turbulent Reynolds stress tensor is needed, it is necessary to postulate a spatial structure of the fluctuations of the electric potential. The periodicity in the toroidal direction allows a Fourier expansion

$$\phi(r,\theta,\varphi,t) = \sum_n \tilde{\phi}_n(r,\theta,t)\exp\left(in\varphi\right) \tag{6}$$

The perturbed electric potential tends to align with the magnetic field. It is characterized by a ballooned poloidal structure, which plays an important role. We therefore adopt the following representation

$$\phi(r,\theta,\varphi,t) = \sum_{\mathbf{k}} \tilde{\phi}_{\mathbf{k}}(r_0,\theta,t)\exp\left\{in\left[\varphi - q(r)\left(\theta-\theta_k\right)\right]\right\} \tag{7}$$

where θ_k measures the departure from up-down symmetry on a given field line $\varphi = q(r)\theta + \alpha$. Non zero values of θ_k result from symmetry breaking mechanisms. The vector $\mathbf{k}$ is a label for the couple (n,θ_k). Therefore the sum over $\mathbf{k}$ designates a summation over the toroidal wave number n and also an integral over a distribution of angles θ_k. The value of the angle θ_k depends on time, as shown by simulations [7]. To some extent, this time dependence can be represented by such a distribution. Quantities labeled with a index $\mathbf{k}$ will be called "Fourier" harmonics, since θ_k can be seen as the Fourier counterpart of the radial variable $nq(r)$. The variable r_0 indicates a slow radial variation, i.e. $r_0 = \varepsilon r$, where $\varepsilon \ll 1$. In practice Eq.(7) offers a local description of turbulence in the neighborhood of a reference radius r_0. All quantities depends on r_0 with a typical scale that is larger than a typical vortex size, but is smaller than a gradient length. The label r_0 is omitted to simplify the notations, unless specified otherwise. Eq.(7) is in principle not acceptable since it is not periodic in θ. Nevertheless it is a reasonable proxy for a turbulence localized on the low field side of a tokamak (i.e. maximum near $\theta = 0$) since $\tilde{\phi}_{\mathbf{k}}(\theta,t)$ is then small for $\theta = \pm\pi$. Hence each Fourier component $\tilde{\phi}_{\mathbf{k}}(\theta,t)$ contains the information on the poloidal localization of fluctuations, and therefore poloidal asymmetries. This formulation is close to the ballooning representation, while θ_k is reminiscent of a ballooning angle [8, 9, 10, 11, 12, 13]. We will keep up with this terminology in the following. As in the ballooning representation, "fast" radial variations comes from the radial dependence of the safety factor $q(r)$ in the exponential argument of Eq.(7), whereas "slow" radial variations come from the amplitude $\tilde{\phi}_{\mathbf{k}}$. We insist on the fact that a "slow" radial scale is not a mean gradient

length - the only constraint is that it should be larger than a distance between resonant surface $\frac{1}{n\frac{dq}{dr}\Big|_{r=r_0}}$.

In the linear picture, a complete mode is given by an integral over the ballooning angle θ_k weighted by an envelope, the width of which is mesoscale and typically scales as $(a\rho_i)^{1/2}$, where a is the minor radius and ρ_i the ion thermal gyroradius radius. Calculating an envelope in turbulent regime has little sense since a global mode has no time to form before turbulent decorrelation occurs, except very close to the threshold. We postulate a Gaussian form for i.e. $\tilde{\phi}_{\mathbf{k}}(\theta,t)$, i.e.

$$\tilde{\phi}_{\mathbf{k}}(\theta,t) = \tilde{\phi}_{\mathbf{k}}(t) a_{\mathbf{k}} \exp\left\{-\frac{1}{2}\alpha_{\mathbf{k}}\left(\theta - \lambda_{\mathbf{k}}\theta_k\right)^2\right\} \tag{8}$$

where $\alpha_{\mathbf{k}}$ and $\lambda_{\mathbf{k}}$ are complex numbers, and $a_{\mathbf{k}}$ is a normalizing factor ($\alpha_{\mathbf{k}}$, $\lambda_{\mathbf{k}}$ and $a_{\mathbf{k}}$ may depend on r_0). This formulation is exact in the linear case, and appears as a reasonable proxy in the non linear regime.

2.1.2 Wave numbers

A reference poloidal wave number is defined as $K_\theta = -\frac{nq(r_0)}{r_0}$. Since transfers of momentum between waves and particles are needed, it is also useful to define effective radial and parallel wave numbers. These wave numbers depend on the poloidal angle. We prefer to use here the Fourier components of these effective wave numbers, defined for each $\mathbf{k}$ as

$$\begin{aligned} K_{r,\mathbf{k}\ell} &= -i\frac{\int_{-\infty}^{\infty} d\theta e^{-i\ell\theta}\frac{\partial\tilde{\phi}_n}{\partial r}\tilde{\phi}_n^*}{\int_{-\infty}^{\infty} d\theta \left|\tilde{\phi}_n\right|^2} \\ K_{\parallel,\mathbf{k}\ell} &= -i\frac{\int_{-\infty}^{\infty} d\theta e^{-i\ell\theta}\frac{1}{qR_0}\frac{\partial\tilde{\phi}_n}{\partial\theta}\tilde{\phi}_n^*}{\int_{-\infty}^{\infty} d\theta \left|\tilde{\phi}_n\right|^2} \end{aligned} \tag{9}$$

The index ℓ is used here instead of the traditional notation m because it is anticipated that the useful values of ℓ are small, typically $\ell = 0, \ell = \pm 1, ...$, and therefore different from the much larger turbulent poloidal wave numbers. Indeed the Fourier components that will be needed are representative of long wavelength poloidal asymmetries. Calculations in Appendix A indicate that the poloidal average radial and parallel wave numbers are of the form

$$K_{r,\mathbf{k}\ell} = C_{r,\mathbf{k}\ell} K_\theta \theta_k \tag{10}$$

$$K_{\parallel,\mathbf{k}\ell} = C_{\parallel,\mathbf{k}\ell} K_\theta \theta_k \tag{11}$$

where $C_{r,\mathbf{k}\ell}$ and $C_{\parallel,\mathbf{k}\ell}$ are numbers, which depend on plasma parameters, and are close to the $\ell = 0$ components for small ballooning angles $\theta_k \ll 1$, i.e.

$$C_{r,\mathbf{k}\ell} = C_{r,\mathbf{k}0} + o\left(\ell^2\theta_k^2\right) \quad (12)$$

$$C_{\parallel,\mathbf{k}\ell} = C_{\parallel,\mathbf{k}0} + o\left(\ell^2\theta_k^2\right) \quad (13)$$

Explicit expressions of the potential structure Eq.(7) are (see Appendix A)

$$C_{r,\mathbf{k}0} = s_0 \frac{\Re(\alpha_\mathbf{k}\delta_\mathbf{k})}{\Re\left(\alpha_\mathbf{k}\right)} \quad (14)$$

$$C_{\parallel,\mathbf{k}0} = \frac{1}{q_0 K_\theta R_0} \left|\alpha_\mathbf{k}\right|^2 \frac{\Im(\delta_\mathbf{k})}{\Re\left(\alpha_\mathbf{k}\right)} \quad (15)$$

where

$$s_0 = \left.\frac{r}{q}\frac{dq}{dr}\right|_{r=r_0} \quad (16)$$

is the magnetic shear calculated at $r = r_0$, $\delta_\mathbf{k} = \lambda_\mathbf{k} - 1$, and $\Re$ (resp. $\Im$) designates the real (resp. imaginary) part of a complex number. In view of the field structure Eq.(8), the real part of $\alpha_\mathbf{k}$ must be positive, i.e. $\Re\left(\alpha_\mathbf{k}\right) \geq 0$, since modes must be spatially localized in the poloidal direction. As expected, the average radial and parallel wave numbers are correlated and proportional to θ_k, which measures the strength of the symmetry breaking mechanism. However a close inspection of Eqs.(14,15) indicates that the proportionality coefficients are not the same. For instance, in the limit $\Re\left(\alpha_\mathbf{k}\right) \gg \Im\left(\alpha_\mathbf{k}\right)$ (non propagative localized mode), it appears that $C_{r,\mathbf{k}0}$ is of the sign of $\Re(\delta_\mathbf{k})s_0$, while $C_{\parallel,\mathbf{k}0}$ is of the sign of $\Im(\delta_\mathbf{k})K_\theta q_0$. Hence the sign and amplitude of the correlation between the poloidally averaged radial and parallel wave numbers is by no way trivial. This relationship has been discussed in [18], in the context of turbulent momentum transport in slab geometry.

2.1.3 Ballooning angle

The value of the ballooning angle θ_k is not easy to determine. In the ballooning formalism, it comes from a calculation of the mode envelope. However, as already mentioned, this calculation is questionable for a turbulent state. An estimate can be found by using a rapid distortion theory [16]. Indeed a structure with initially a zero ballooning angle $\theta_k = 0$ will acquire an effective radial wave number due to a shear flow that is equal to $\theta_k = -\frac{1}{s_0}V_E' t$ after a time t. Here V_E' is the shear flow rate, i.e. the radial derivative of the mean ExB velocity. Defining a correlation time τ_c, one gets the following estimate

$$\theta_k = -\frac{1}{s_0} V_E' \tau_c \quad (17)$$

Other expressions of θ_k have been given in the past [10, 11, 12, 13, 17], with similar structures as Eq.(17) when envelopes are spatially localized. The exact expression of θ_k has no real importance here, since we are interested in the relative signs and amplitudes of the momentum fluxes. Sources of symmetry breaking different from shear flow will lead to different expressions of θ_k, but will cause correlated radial and parallel wavenumbers.

2.2 $E \times B$ drift stress tensor

We estimate now the radial fluxes of poloidal and parallel momentum due to $E \times B$ drift, which are proportional to the corresponding components of the Reynolds stress

$$\Pi^E_{r\theta}(\theta,t) = \frac{1}{N}\int_0^{2\pi}\frac{d\varphi}{2\pi}\int d^3\mathbf{v} F v_{Er} v_{E\theta} \tag{18}$$

$$\Pi^E_{r\|}(\theta,t) = \frac{1}{N}\int_0^{2\pi}\frac{d\varphi}{2\pi}\int d^3\mathbf{v} F v_{Er} v_{\|} \tag{19}$$

The distribution function is decomposed in the same way as the potential

$$F(r,\theta,\varphi,v_\|,\mu,t) = \sum_{\mathbf{k}} F_{\mathbf{k}}(\theta,v_\|,\mu,t)\exp\left\{in\left[\varphi - q(r)\left(\theta-\theta_k\right)\right]\right\} \tag{20}$$

where $\mu = \frac{mv_\perp^2}{2B}$ is the adiabatic invariant. The equations Eqs.(18,19) can then be recast as

$$\Pi^E_{r\theta}(\theta,t) = -\sum_{\mathbf{k}} \mathcal{A}_{\mathbf{k}}(\theta) s_0(\theta-\theta_k)\left|v_{E\mathbf{k}}(t)\right|^2 \tag{21}$$

$$\Pi^E_{r\|}(\theta,t) = \sum_{\mathbf{k}} \mathcal{A}_{\mathbf{k}}(\theta) v^*_{E\mathbf{k}}(t) V_{\|\mathbf{k}}(t) \tag{22}$$

where

$$V_{\|\mathbf{k}} = \frac{1}{N}\int d^3\mathbf{v} F_{\mathbf{k}} v_\| \tag{23}$$

is the Fourier component of the parallel fluid velocity and

$$v_{E\mathbf{k}} = -iK_\theta \frac{\tilde{\phi}_{\mathbf{k}}}{B_0} \tag{24}$$

is the Fourier component of the radial component of the $E\times B$ drift velocity. The poloidal structure function $\mathcal{A}_{\mathbf{k}}(\theta)$ is defined as (see details in Appendix A)

$$\mathcal{A}_{\mathbf{k}}(\theta) = \lim_{\theta_k\to 0}\frac{\left|\tilde{\phi}_{\mathbf{k}}(\theta,t)\right|^2}{\left|\phi_{\mathbf{k}}(t)\right|^2} \tag{25}$$

$$\int_{-\infty}^{\infty} d\theta \mathcal{A}_{\mathbf{k}}^2(\theta) = 1 \tag{26}$$

The amplitude $\mathcal{A}_{\mathbf{k}}$ does not depend on time for the structure Eq.(7). Note that at this stage, the fluxes depend on the poloidal angle and time (plus a slow radial variation in r_0). A rough estimate of $V_{\|\mathbf{k}}$ is obtained by a rapid distortion argument [16], i.e. $V_{\|\mathbf{k}} \simeq -iK_{\|}\frac{e}{m}\tilde{\phi}_{\mathbf{k}}\tau_{\mathbf{k}}$, where $\tau_{\mathbf{k}}$ is a correlation time. The components of the Reynolds stress can be expanded as Fourier series in the poloidal direction

$$\Pi_{r\theta}^E(\theta,t) = \sum_{\ell=-\infty}^{+\infty} \Pi_{r\theta,\ell}^E(t) e^{i\ell\theta} \tag{27}$$

$$\Pi_{r\|}^E(\theta,t) = \sum_{\ell=-\infty}^{+\infty} \Pi_{r\|,\ell}^E(t) e^{i\ell\theta} \tag{28}$$

Using the expressions Eqs.(10,11), one finds

$$\Pi_{r\theta,\ell}^E(t) = -\sum_{\mathbf{k}} C_{r,\mathbf{k}\ell} \left|v_{E\mathbf{k}}(t)\right|^2 \theta_k \tag{29}$$

$$\Pi_{r\|,\ell}^E(t) = \sum_{\mathbf{k}} C_{\|,\mathbf{k}\ell}\omega_c\tau_{\mathbf{k}} \left|v_{E\mathbf{k}}(t)\right|^2 \theta_k \tag{30}$$

where $\omega_c = \frac{eB_0}{m} > 0$ is the cyclotron pulsation. The components $C_{r,\mathbf{k}\ell}$ and $C_{\|,\mathbf{k}\ell}$ are even functions of ℓ, i.e.

$$\begin{aligned} C_{r,\mathbf{k},-\ell} &= C_{r,\mathbf{k}\ell} \\ C_{\|,\mathbf{k},-\ell} &= C_{\|,\mathbf{k}\ell} \end{aligned} \tag{31}$$

so that $\Pi_{r\theta}^E(\theta,t)$ and $\Pi_{r\|}^E(\theta,t)$ are even functions of θ. This is because the ballooning angle is supposed to be small $\theta_k \ll 1$, and calculations are run at order one in θ_k.

Since we are interested in signs, a rapid distortion theory may not be accurate enough. A quasi-linear theory provides a more precise value of the time and poloidal average of $\Pi_{r\|}^E$. The calculation is done in Appendix B, and confirms the estimate Eq.(30). The structure of the later is in line with previous calculations of the residual stress (see [19, 20, 21], and overviews [22, 23]). The structure of the flux of poloidal momentum Eq.(29) is well-known [25] and was used abundantly in the context of transport barrier formation. We note that $\Pi_{r\theta,\ell}^E$ and $\Pi_{r\|,\ell}^E$ are anti-correlated when $C_{r,\mathbf{k}\ell}$ and $C_{\|,\mathbf{k}\ell}$ are of the same sign.

3 Flux of parallel momentum due to curvature drift

The expression Eq.(2) of the radial flux of parallel momentum due to curvature shows that a finite flux can only be due to up-down symmetries of the distribution function. The rationale here is as follows: because turbulence is ballooned, the stress tensor is ballooned too, thus leading to poloidal asymmetries of the poloidal flow, and therefore of the electric potential. The resulting distorted distribution function is correlated with the $E \times B$ Reynolds stress, and therefore with the $E \times B$ radial flux of parallel momentum.

3.1 Generation of $E \times B$ poloidal convective cells

Damping of time dependent and poloidally asymmetric flows is not primarily due to collisions, but rather wave particle resonant effects. An estimate can be obtained by solving the linear gyrokinetic equation

$$\begin{aligned} \frac{\partial G}{\partial t} &+ \mathbf{v}_E \cdot \nabla G + \mathbf{v}_D \cdot \nabla G + v_\parallel \nabla_\parallel G = \\ & F_M \left(\frac{\partial}{\partial t} + \mathbf{v}_* \cdot \nabla \right) \frac{e}{T} \left(\mathcal{J} \cdot \phi \right) \end{aligned} \tag{32}$$

coupled to the Poisson equation

$$-\nabla \cdot \left(\frac{Nm}{B^2} \nabla_\perp \right) \phi + \frac{Ne^2}{T} \left(\phi - \langle \phi \rangle_\psi \right) = e \int d^3\mathbf{v} \mathcal{J} \cdot (F - F_M) \tag{33}$$

where N is the unperturbed density, $\mathcal{J}$ the gyroaverage operator, $\mathbf{v}_* = \frac{T}{eB_0} \frac{\partial \ln F_M}{\partial r}$ the kinetic diamagnetic velocity, F_M is the unshifted Maxwellian distribution function built with the density N and temperature T, and $G = F - F_M + F_M \frac{e\phi}{T}$ is the non adiabatic part of the distribution function. The distribution functions F and G are functions of the gyrocenter-center position, the adiabatic invariant μ and parallel velocity $v_\parallel$. The parallel non linear term has been neglected. The mirror force is also ignored since the quantity of interest is the ion parallel flux, to which passing particles contribute mot. To assess the large scale flow dynamics, the limit $\mathcal{J} \to 1$ can be safely kept. For non zonal modes $\langle \phi \rangle_\psi = 0$, this gives an equation for the potential vorticity $\phi - \rho_i^2 \nabla_\perp^2 \phi$, i.e.

$$\begin{aligned} & N \left(\frac{\partial}{\partial t} + \mathbf{v}_E \cdot \nabla \right) \left(1 - \rho_i^2 \nabla_\perp^2 \right) \frac{e\phi}{T} \\ + \quad & \nabla_\parallel \Gamma_\parallel + \nabla \cdot \left(N \mathbf{v}_E + N \mathbf{v}_{*p} \right) = 0 \end{aligned} \tag{34}$$

where $\Gamma_\parallel$ is the ion parallel flux, and $\mathbf{v}_{*p}$ the diamagnetic velocity. The vorticity equation Eq.(34) has been derived by assuming that the electric potential wavelength is smaller than the gradient lengths of density and temperature. The axisymmetric electric potential $n = 0$ is Fourier expanded in poloidal angle and time

$$\phi_{n=0}(\theta, t) = \sum_{\ell\omega} \phi_{\ell\omega} exp\left\{i\left(\ell\theta - \omega t\right)\right\} \tag{35}$$

where $\ell \neq 0$ since zonal flows are excluded. One can show the following variant of the Taylor identity [24] (see Appendix C)

$$\frac{1}{B_0}\int_0^{2\pi} \frac{d\varphi}{2\pi} \left(\mathbf{v}_E \cdot \nabla\right) \nabla_\perp^2 \phi = \nabla_\perp^2 \Pi_{r\theta}^E \tag{36}$$

where

$$\nabla_\perp^2 \Pi_{r\theta}^E = \frac{1}{r_0}\frac{\partial}{\partial r_0}\left(r_0 \frac{\partial}{\partial r_0}\Pi_{r\theta}^E\right) \tag{37}$$

It is reminded that r_0 is the reference radius in the neighborhood of which the calculations are performed. A subsidiary small parameter $\rho_\pi = \frac{\rho_i}{\lambda_\pi} < 1$ is introduced at this point, which is the ratio of the thermal Larmor radius to the typical radial wavelength of the turbulent Reynolds stress tensor. Only terms of order ρ_π^2 are retained in the following.

The divergence of the parallel flux in the vorticity equation Eq.(34) can be calculated by computing the axisymmetric components $n = 0, \ell \neq 0$ of the perturbed distribution function, which is a linear solution of the gyrokinetic equation Eq.(32), i.e.

$$G_{\ell\omega} = F_M \frac{\omega}{\omega - \ell\frac{v_\parallel}{q_0 R_0} + i0^+}\frac{e\phi_{\ell\omega}}{T} \tag{38}$$

It appears that the ℓ component of the parallel flux divergence is

$$\left\{\nabla_\parallel \left[\int d^3\mathbf{v} v_\parallel F\right]\right\}_\ell = -i\omega\left(\sigma_{\ell\omega} + i\nu_{\ell\omega}\right)\frac{e\phi_{\ell\omega}}{T} \tag{39}$$

where $\sigma_{\ell\omega}\omega$ is a frequency shift and $\nu_{\ell\omega}\omega$ is the flow damping rate ($\nu_{\ell\omega}\omega > 0$). The explicit expressions of $\sigma_{\ell\omega}$ and $\nu_{\ell\omega}$ are

$$\sigma_{\ell\omega} = P.P.\frac{1}{(2\pi)^{1/2}}\int_{-\infty}^{+\infty} d\zeta e^{-\frac{\zeta^2}{2}} \frac{-\ell\frac{v_{Ti}}{q_0 R_0}\zeta}{\omega - \ell\frac{v_{Ti}}{q_0 R_0}\zeta + i0^+} \tag{40}$$

and

$$\nu_{\ell\omega} = \left(\frac{\pi}{2}\right)^{1/2}\frac{\omega}{|\ell|\,\omega_t} e^{-\frac{\omega^2}{2\ell^2\omega_t^2}} \tag{41}$$

where $\omega_t = \left|\frac{v_{Ti}}{q_0 R_0}\right|$ is a thermal transit frequency. Some useful properties are

$$\begin{array}{ll} \sigma_{-\ell\omega} = \sigma_{\ell\omega} & \nu_{-\ell\omega} = \nu_{\ell\omega} \\ \sigma_{-\ell-\omega} = \sigma_{\ell\omega} & \nu_{-\ell-\omega} = -\nu_{\ell\omega} \end{array} \tag{42}$$

The last term in the vorticity equation Eq.(34) cancels out since the divergence of the diamagnetic current term is linear so that its toroidal average is zero. The other term is a particle flux which is equal to zero for an ITG turbulence. The vorticity equation Eq.(34) can then be solved by combining the Taylor identity Eq.(36) with the parallel flow divergence Eq.(39), thus providing the Fourier components of the electric potential $\phi_{\ell\omega}$

$$\frac{\phi_{\ell\omega}}{B} = -\frac{K_{\perp,\ell}^2 \rho_i^2}{1 + \sigma_{\ell\omega} + i\nu_{\ell\omega}} \frac{\Pi_{r\theta,\ell\omega}^E}{-i\omega} \tag{43}$$

where the Reynolds stress tensor has been expanded in a Fourier series

$$\Pi_{r\theta}^E(\theta, t) = \sum_{\ell\omega} \Pi_{r\theta,\ell\omega}^E exp\left\{i\left(\ell\theta - \omega t\right)\right\} \tag{44}$$

and $K_{\perp,\ell}^2$ has to be understood as an operator that acts on $\Pi_{r\theta,\ell\omega}^E$, $K_{\perp,\ell}^2 \Pi_{r\theta,\ell\omega}^E = -\nabla_\perp^2 \Pi_{r\theta,\ell\omega}^E$. It is reminded that only the leading term in $\rho_\pi^2 \simeq K_{\perp,\ell}^2 \rho_i^2$ is kept.

The expression of the electric potential Fourier components Eq.(43) is of central interest since it provides the structure of time-dependent poloidal convective cells which are driven by turbulent eddies. Hence it calls for several comments:

1. Using the properties Eq.(42), it appears that $\phi_{\ell\omega}^* = \phi_{-\ell-\omega}$, as expected. However, even if the stress tensor is up-down symmetrical at lowest order in ballooning angle, i.e. $\Pi_{r\theta,-\ell\omega}^E = \Pi_{r\theta,\ell\omega}^E$ (a consequence of Eq.(31)), this is not the case for the potential, which develops up-down asymmetries $\phi_{-\ell\omega} \neq \phi_{\ell\omega}$, due to damping.

2. Poloidal convective cells are Landau damped due to their finite poloidal wave number, as expected. However it appears that their damping rate is small at low frequencies, hence favoring their onset and sustainment. This result can be understood as follows : for a steady axisymmetric potential ($\omega = 0, n = 0$) the 3 invariants of motion (energy, kinetic toroidal momentum, adiabatic invariant) are preserved, so that the motion is integrable and no damping is possible is the distribution function is smooth in the phase space. It will be seen in the next section

that the $1/\omega$ scaling of their amplitude plays an important role in the generation of parallel flow via curvature drift. At very low frequencies however, collisions take over, thus regularizing the infrared singularity.

3. The value of $K_{\perp,\ell}\rho_i \simeq \rho_\pi$ is of central importance. First, it is assumed that $K^2_{\perp,\ell}\rho_i^2$ is positive, i.e. we consider here the case of radial oscillations of the Reynolds stress. Secondly, the mechanism presented here requires values of ρ_π that are not too small, i.e. corrugations of the Reynolds stress with a spatial scale of a few gyroradii [3, 6, 7]. This may push the present model to its validity limit, since it was assumed that the variation with r_0 correspond to scales larger than the distance between resonant surfaces, itself of the order of the ion gyroradius. A more accurate calculation for $\rho_\pi \simeq 1$ is intricate as it requires a more precise procedure to solve the vorticity equation, as done for zonal flows ([26] and references therein).

4. The ordering of gyrokinetic theory is not broken since the amplitude of the normalized potential $\frac{e\phi_{\ell\omega}}{T_i}$ remains small, of the order of ρ_*. This can be verified by using Eq.(43) , and noting that the turbulence stress tensor scales as $\rho_*^2 v_T^2$, frequencies as $\frac{v_T}{R}$ so that $\frac{e\phi_{\ell\omega}}{T_i} \simeq \rho_\pi^2 \rho_*$. Macroscopic flows $\rho_\pi \simeq \rho_*$ would lead to very small amplitudes of the potential turbulence on the electric potential $\frac{e\phi_{\ell\omega}}{T_i} \simeq \rho_*^3$ with a negligible effect, as discussed in [4]. Numerical simulations suggest that ρ_π is rather in the range of 0.1 [6].

3.2 Curvature driven flux of parallel momentum

The banana-plateau component of the neoclassical flux of parallel momentum is known to cancel. Obviously the Pfirsch-Schlüter contribution vanishes too in the collisionless regime so that the overall standard neoclassical momentum flux is null [27, 28, 29] (see [30] for an overview). Therefore one is left with the cross-correlation between the curvature drift and the perturbed distribution function due to the electric potential fluctuations $\phi_{\ell\omega}$ driven by turbulent eddies. This cross-correlation is responsible for a finite flux of parallel momentum. The time dependent radial flux of parallel momentum due to curvature

drift reads

$$\begin{aligned}\left\langle \Pi^D_{r\|} \right\rangle_\theta &= \frac{1}{N}\int_0^{2\pi}\frac{d\varphi}{2\pi}\int_0^{2\pi}\frac{d\theta}{2\pi}\int d^3\mathbf{v} F v_{Dr} v_\| \\ &= \sum_{\ell=-\infty}^{+\infty}\int d^3\mathbf{v} v_\| F_\ell v^*_{Dr\ell} \end{aligned} \tag{45}$$

Here v_{Dr} is the geodesic component of the curvature drift velocity

$$v_{Dr} = v_D \frac{1}{2i}\left(\delta_{\ell,1} - \delta_{\ell,-1}\right) \tag{46}$$

where

$$v_D = -\frac{\mu B_0 + m v_\|^2}{e B_0 R_0} \tag{47}$$

We compute the momentum flux by using again the linear solution Eq.(38) of the gyrokinetic equation Eq.(32). The frequency Fourier components of the parallel momentum flux Eq.(45) read

$$\begin{aligned}\left\langle \Pi^D_{r\|\omega} \right\rangle_\theta &= -q_0 \sum_{\ell=\pm 1}\int_{-\infty}^{+\infty}\frac{d\zeta}{(2\pi)^{1/2}} e^{-\frac{\zeta^2}{2}} \frac{-\ell\frac{v_{Ti}}{q_0 R_0}\zeta}{\omega - \ell\frac{v_{Ti}}{q_0 R_0}\zeta + i0^+} \\ &\left(1+\zeta^2\right)\frac{1}{2}\left(\delta_{\ell,1}+\delta_{\ell,-1}\right)\frac{-i\omega\phi_{\ell\omega}}{B}\end{aligned} \tag{48}$$

Using Eq.(39) (or equivalently Eqs.(41,40)), the integral over the velocity can be expressed as a function of $\sigma_{\ell\omega}$ and $\nu_{\ell\omega}$, namely

$$\begin{aligned}\left\langle \Pi^D_{r\|\omega} \right\rangle_\theta &= -q_0 \sum_{\ell=\pm 1}\left[1 + \left(1+\frac{\omega^2}{\omega_t^2}\right)\left(\sigma_{\ell\omega} + i\nu_{\ell\omega}\right)\right] \\ &\frac{1}{2}\left(\delta_{\ell,1}+\delta_{\ell,-1}\right)\frac{-i\omega\phi_{\ell\omega}}{B}\end{aligned} \tag{49}$$

We note that it is essential to deal with time dependent perturbations to get a finite flux. Static perturbations resonate at zero parallel velocity $v_\| = 0$ and therefore do not contribute to the flux of parallel momentum. This is the basic reason why the banana-plateau neoclassical flux of parallel momentum is zero. In the present case, this cancellation is prevented by the increase of the potential amplitude at low frequency, as shown by the expression of $\phi_{\ell\omega}$ Eq.(43). In other words, it is the time derivative of the electric potential that matters. Eq.(49) combined with Eq.(43) leads to the following expression of the time Fourier transform of the momentum flux

$$\left\langle \Pi^D_{r\|\omega} \right\rangle_\theta = q_0 \frac{1 + \left(1+\frac{\omega^2}{\omega_t^2}\right)\left(\sigma_{\ell\omega} + i\nu_{\ell\omega}\right)}{1 + \sigma_{\ell\omega} + i\nu_{\ell\omega}} K^2_{\perp,1}\rho_i^2 \Pi^E_{r\theta,1\omega} \tag{50}$$

where the up-down symmetry of the turbulent Reynolds stress $\Pi^E_{r\theta,-1\omega} = \Pi^E_{r\theta,1\omega}$ has been used (consequence of Eq.(31). The next step consists in taking the zero frequency limit of Eq.(50), which is equivalent to a time average. For frequencies lower than the transit frequency, $\omega \ll \omega_t$, the frequency shift is close to unity, $\sigma_{\ell\omega} = 1 + o(\omega^2/\omega_t^2)$, while the damping rate $\nu_{\ell\omega} \simeq \omega/\omega_t$ vanishes. The expression Eq.(50) becomes remarkably simple

$$\left\langle \Pi^D_{r\|} \right\rangle_{\theta,t} = -q_0 \left\langle \cos(\theta)\, \rho_i^2 \nabla_\perp^2 \Pi^E_{r\theta} \right\rangle_{\theta,t} \tag{51}$$

For a ballooned turbulence, the Reynolds stress is ballooned too. If fluctuations are strongly localized on the low field side, the prefactor $\cos(\theta)$ can be replaced by 1 in Eq.(51). This can also be demonstrated by using the structure of the stress tensor Eq.(29) and the expression of $C_{r,\mathbf{k}\ell}$ with ℓ (see Eq.(12)), which allows replacing $\Pi^E_{r\theta,1\omega}$ by $\Pi^E_{r\theta,0\omega}$ at low values of the ballooning angle, where $\Pi^E_{r\theta,0\omega}$ is the poloidal average $\ell = 0$ of the $E \times B$ Reynolds stress.

The reader may actually be surprised by the result Eq.(51), which is quite simple. One may actually wonder whether a more direct calculation of $\Pi^D_{r\|}$ is possible, and indeed it is. Since the parallel velocity plays a subdominant role in the curvature drift, essentially because the resonant velocity goes like the pulsation, the curvature driven flux of momentum Eq.(45) can be reformulated as

$$\left\langle \Pi^D_{r\|} \right\rangle_{\theta,t} = -\frac{T}{NeB_0R_0} \int_0^{2\pi} \frac{d\varphi}{2\pi} \int_0^{2\pi} \frac{d\theta}{2\pi} \sin(\theta) \Gamma_\| \tag{52}$$

An integration by part allows a reformulation in terms of the parallel gradient of the parallel flux

$$\left\langle \Pi^D_{r\|} \right\rangle_{\theta,t} = -q_0 \frac{T}{NeB_0} \int_0^{2\pi} \frac{d\varphi}{2\pi} \int_0^{2\pi} \frac{d\theta}{2\pi} \cos(\theta) \nabla_\| \Gamma_\| \tag{53}$$

Using the vorticity equation Eq.(34), and the Taylor identity Eq.(36), one finds Eq.(51). It is quite remarkable that this result does not depend on the details of the poloidal convective cells, which act as mediators. Their emergence in simulations is nevertheless essential to this process. An example of turbulence self-organization via the generation of poloidal convective cells is shown in Fig.3. This figure comes from simulations run with the GYSELA gyrokinetic code [31]. It turns out that poloidal convective cells play also a role in the interplay between turbulent and neoclassical impurity transport [15].

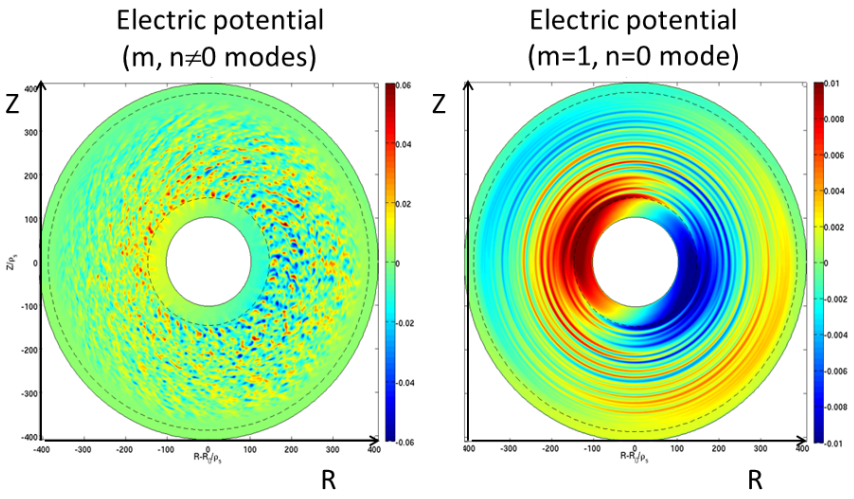

Figure 3: Small scale eddies and poloidal convective cells in a GYSELA simulation.

4 Comparison of $E \times B$ and curvature driven momentum fluxes

4.1 General expressions of momentum fluxes fluxes

The expression Eq.(51) of the radial flux of parallel momentum due to the curvature drift can be expressed in the Fourier space using Eq.(29)

$$\left\langle \Pi^D_{r\|} \right\rangle_{\theta,t} = -q_0 \sum_{\mathbf{k}} C_{r,\mathbf{k}0} K^2_{\perp,\ell} \rho_i^2 \left\langle |v_{E\mathbf{k}}|^2 \right\rangle_t \theta_k \tag{54}$$

This expression can be compared with the $E \times B$ flux of momentum Eq.(84)

$$\left\langle \Pi^E_{r\|} \right\rangle_{\theta,t} = \sum_{\mathbf{k}} \omega_c \tau_{\mathbf{k}} C_{\|,\mathbf{k}0} \left\langle |v_{E\mathbf{k}}|^2 \right\rangle_t \theta_k \tag{55}$$

It appears that these two components of the total flux of parallel momentum are anti-correlated when $C_{r,\mathbf{k}0}$ and $C_{\|,\mathbf{k}0}$ are of the same sign (for positive q_0). This is also the condition for anti-correlation of the $E \times B$ poloidal and parallel components of the Reynolds stress. This is the main result of this paper. The final answer is clearly sensitive to processes that determine the radial and parallel wavelengths,

which are presumably determined by non linear effects. Nevertheless it is interesting to calculate the linear values of $C_{r\mathbf{k}}$ and $C_{\|\mathbf{k}}$, and the corresponding sign of the correlation.

4.2 Application to Ion Temperature Gradient driven turbulence

An instructive example is the case of an unstable linear toroidal Ion Temperature Gradient (ITG) driven mode. General expressions of $C_{r\mathbf{k}}$ and $C_{\|\mathbf{k}}$ are derived in the hydrodynamic limit in the Appendix D. In the long wavelength limit $K_\theta^2 \rho_i^2 \ll 1/s_0^2$ and strong magnetic shear $|s_0| \gg 1$, explicit expressions of the coefficients $C_{r,\mathbf{k}0}$ and $C_{\|,\mathbf{k}0}$ can be found

$$C_{r,\mathbf{k}0} = c_{r\mathbf{k}} s_0 \tag{56}$$

$$C_{\|,\mathbf{k}0} = c_{\|\mathbf{k}} \frac{\rho_i}{R_0} \left(K_\theta \rho_i s_0\right)^2 q_0 s_0 \tag{57}$$

The numbers $c_{r\mathbf{k}}$ and $c_{\|\mathbf{k}}$ depend on the normalized frequencies $\frac{\omega_\mathbf{k}}{\omega_d}$ and $\frac{\gamma_\mathbf{k}}{\omega_d}$ only, where $\omega_\mathbf{k}$ and $\gamma_\mathbf{k}$ are the real and imaginary parts of the linear frequency in the plasma frame (frame where the local radial electric field is zero), and

$$\omega_d = -2 \frac{K_\theta T}{e B_0 R_0} \tag{58}$$

is a thermal magnetic field curvature frequency. More precisely

$$c_{r\mathbf{k}} = \frac{1}{2} \frac{1}{\left(1 + \frac{\gamma_\mathbf{k}^2}{\omega_\mathbf{k}^2}\right)^{1/2}} \left(\lambda_- - \mathrm{sgn}\left(\omega_\mathbf{k} \omega_d s_0\right)\right) \tag{59}$$

$$c_{\|\mathbf{k}} = 2^{1/2} \frac{1}{|q_0|} \left|\frac{\omega_\mathbf{k}}{\omega_d s_0}\right|^{3/2} \left(1 + \frac{\gamma_\mathbf{k}^2}{\omega_\mathbf{k}^2}\right)^{1/2} \lambda_-^{1/2} \tag{60}$$

and

$$\lambda_- = \left[\left(1 + \frac{\gamma_\mathbf{k}^2}{\omega_\mathbf{k}^2}\right)^{1/2} - \mathrm{sgn}\left(\omega_\mathbf{k} \omega_d s_0\right)\right] \tag{61}$$

The coefficient λ_- is always positive. These expressions are valid for any sign of q_0 and s_0. We now restrict the discussion to the generic case $q_0 > 0$ and $s_0 > 0$. These considerations lead to the following estimates of the momentum fluxes

$$\left\langle \Pi_{r\|}^D \right\rangle_{\theta,t} \simeq s_0 q_0 \sum_\mathbf{k} c_{r\mathbf{k}} \left(K_{\perp,1} \rho_i\right)^2 \left\langle |v_{E\mathbf{k}}|^2 \right\rangle_t \theta_k \tag{62}$$

and

$$\left\langle \Pi^E_{r\|} \right\rangle_{\theta,t} \simeq -s_0 q_0 \sum_{\mathbf{k}} c_{\|\mathbf{k}} \omega_t \tau_{\mathbf{k}} \left(K_\theta \rho_i s_0\right)^2 \left\langle \left|v_{E\mathbf{k}}\right|^2 \right\rangle_t \theta_k \qquad (63)$$

For $\omega_{\mathbf{k}} \simeq \gamma_{\mathbf{k}} \simeq \omega_d$, the two numbers $c_{r\mathbf{k}}$ and $c_{\|\mathbf{k}}$ are of the same order of magnitude. The two fluxes are therefore comparable when $K_{\perp,1}\rho_i \simeq \rho_\pi \simeq K_\theta \rho_i \left(\omega_t \tau_{\mathbf{k}}\right)^{1/2}$. This condition appears as reasonable since the intensity wave number spectrum typically peaks at $K_\theta \rho_i \simeq 0.1$, provided $\omega_t \tau_{\mathbf{k}} \simeq o(1)$ [32, 33] .

Regarding the signs, it appears that for modes that drift in the ion diamagnetic direction $\mathrm{sgn}\left(\omega_{\mathbf{k}}\omega_d\right) = 1$, $c_{r\mathbf{k}}$ is negative for a weak drive $\gamma_{\mathbf{k}} \ll \omega_{\mathbf{k}}$, and positive for strong drive $\gamma_{\mathbf{k}} \geq \omega_{\mathbf{k}}$. Since $c_{\|\mathbf{k}}$ is always positive, this means that $C_{\|,\mathbf{k}0}$ and $C_{r,\mathbf{k}0}$ are positively correlated near threshold, and anti-correlated far from threshold. Consequently the two fluxes or parallel momentum are *positively correlated* for low drive $\gamma_{\mathbf{k}} \ll \omega_{\mathbf{k}}$ and *anti-correlated* for strong drive $\gamma_{\mathbf{k}} \geq \omega_{\mathbf{k}}$. For modes drifting in the electron diamagnetic direction, $\mathrm{sgn}\left(\omega_{\mathbf{k}}\omega_d\right) = -1$, anti-correlation always occurs. For ITG modes, drift in the ion diamagnetic direction is expected, so that anti-correlation is expected only far enough from the instability threshold. It is not clear whether this finding agrees or not with previous numerical findings for momentum transport [6, 7]. Nevertheless it is stressed that the hydrodynamic limit that is being used here, is a rather demanding approximation that becomes correct well above the instability threshold, i.e. for $\gamma_{\mathbf{k}} > \omega_{\mathbf{k}}$. This is precisely the regime where an agreement with simulations is found, i.e. anticorrelation. In that regard some further analysis of the numerical simulations would be helpful. An encouraging observation though [7] is that the $E \times B$ flux of parallel momentum is anti-correlated with the ballooning angle θ_k, which suggests positive $c_{\|\mathbf{k}}$ in view of Eq.(63). Moreover, it is possible (if not likely) that the two terms $c_{r\mathbf{k}}$ and $c_{\|\mathbf{k}}$ are determined by non linear processes and not well captured by a linear analysis.

5 Conclusion

It is shown here that the $E \times B$ Reynolds stress tensor generates poloidal asymmetries of the plasma flow due to turbulence ballooning. These poloidal convective cells are weakly damped at low frequency. Their radial scale is dictated by the turbulent Reynolds stress, and their poloidal wavenumbers are small. These cells drive up-down asymmetries of the distribution function, which are responsible for a non-zero radial flux of parallel momentum due to the geodesic component of the particle curvature drift. The entire process requires a symmetry breaking mechanism, for instance a mean shear flow. Since

the turbulent Reynolds can be seen as a flux of momentum, it appears that the two components of the radial flux of parallel momentum due to curvature and $E \times B$ drift are correlated. This general result comes from a simple relationship between the momentum flux due to curvature and the turbulent Reynolds stress. Although poloidal convective cells do not appear explicitly in this relationship, they play an essential role in this mechanism. A analytic calculation shows that anti-correlation between the components of the turbulent Reynolds stress results in anti-correlation of the two contributions to the flux of parallel momentum that come from $E \times B$ and curvature drifts. A quasi-linear calculation of all quantities, based on ITG linear stability indicates that positive correlation is expected near threshold, and anti-correlation for strong drive. Hence no firm conclusion can be drawn as to the relevance of this mechanism to explain the numerical results. Nevertheless the fact that the hydrodynamic limit that has been used is only valid well above the stability threshold, i.e. strong drive, is encouraging since it is the case where anti-correlation is found, in agreement with numerical findings. It is likely that poloidal convective cells generated by turbulence have other consequences on turbulent transport and turbulence. Indeed they may participate in turbulence self-regulation via vortex shearing processes similar to zonal flows.

APPENDICES

A Mode structure

The mode structure Eq.(8) lead to a turbulence intensity that reads

$$\left|\tilde{\phi}_{\mathbf{k}}(\theta,t)\right|^2 = \left|\phi_{\mathbf{k}}(t)\right|^2 \mathcal{A}_{\mathbf{k}}(\theta) \tag{64}$$

where $\mathcal{A}_{\mathbf{k}}(\theta)$ is a form factor

$$\mathcal{A}_{\mathbf{k}}(\theta) = \left(\frac{\bar{\alpha}_{\mathbf{k}}}{\pi}\right)^{1/2} \exp\left\{-\bar{\alpha}_{\mathbf{k}}\left(\theta - \bar{\lambda}_{\mathbf{k}}\theta_k\right)^2\right\} \tag{65}$$

and

$$\begin{aligned} \bar{\alpha}_{\mathbf{k}} &= \frac{1}{2}\left(\alpha_{\mathbf{k}} + \alpha_{\mathbf{k}}^*\right) = \Re\left(\alpha_{\mathbf{k}}\right) \\ \bar{\lambda}_{\mathbf{k}} &= \frac{\alpha_{\mathbf{k}}\lambda_{\mathbf{k}} + \alpha_{\mathbf{k}}^*\lambda_{\mathbf{k}}^*}{\alpha_{\mathbf{k}} + \alpha_{\mathbf{k}}^*} = \frac{\Re(\alpha_{\mathbf{k}}\lambda_{\mathbf{k}})}{\Re\left(\alpha_{\mathbf{k}}\right)} \end{aligned} \tag{66}$$

The amplitude $a_{\mathbf{k}}$ in Eq.(8) has been chosen such that

$$\int_{-\infty}^{\infty} d\theta \left|\tilde{\phi}_{\mathbf{k}}(\theta,t)\right|^2 = \left|\tilde{\phi}_{\mathbf{k}}(t)\right|^2 \tag{67}$$

namely

$$a_{\mathbf{k}} = \left(\frac{\bar{\alpha}_{\mathbf{k}}}{\pi}\right)^{1/4} exp\left\{\frac{|\alpha_{\mathbf{k}}|^2}{2\left(\alpha_{\mathbf{k}}+\alpha_{\mathbf{k}}^*\right)}\left(\lambda_{\mathbf{k}}-\lambda_{\mathbf{k}}^*\right)^2\right\} \tag{68}$$

The poloidal Fourier components of the radial and parallel wave numbers Eq.(9) and Eq.(10) can then be recast as

$$\begin{aligned} K_{r,\mathbf{k}\ell} &= K_\theta s_0 \int_{-\infty}^{\infty} d\theta e^{-im\theta}\left(\theta-\theta_k\right)\mathcal{A}_{\mathbf{k}}(\theta) \\ K_{\parallel,\mathbf{k}\ell} &= \frac{1}{q_0 R_0}\int_{-\infty}^{\infty} d\theta e^{-im\theta}\left(\theta-\lambda_{\mathbf{k}}\theta_k\right)\mathcal{A}_{\mathbf{k}}(\theta) \end{aligned} \tag{69}$$

For a strongly ballooned turbulence $\alpha_{\mathbf{k}} \gg 1$, and small values of the ballooning angle $\theta_k \ll 1$, one gets at first order in θ_k

$$K_{r,\mathbf{k}\ell} = K_{r,0} = K_\theta s_0 \frac{\Re(\alpha_{\mathbf{k}}\delta_{\mathbf{k}})}{\Re\left(\alpha_{\mathbf{k}}\right)}\theta_k \tag{70}$$

$$K_{\parallel,\mathbf{k}\ell} = K_{\parallel,0} = \frac{|\alpha_{\mathbf{k}}|^2}{q_0 R_0}\frac{\Im(\delta_{\mathbf{k}})}{\Re\left(\alpha_{\mathbf{k}}\right)}\theta_k \tag{71}$$

where $\delta_{\mathbf{k}} = \lambda_{\mathbf{k}} - 1$. Hee $\Re(z)$ and $\Im(z)$ indicate the real and imaginary parts of a complex number z.

B Quasilinear expression of $E \times B$ momentum flux

We start from the expression of the $E \times B$ drift contribution to the momentum flux, and readily get its time average Eq.(19)

$$\left\langle \Pi_{r\parallel}^E(\theta,t)\right\rangle_t = \frac{1}{N}\sum_{\mathbf{k}\omega}\int d^3\mathbf{v}\tilde{F}_{\mathbf{k}\omega}v_\parallel\tilde{v}_{E\mathbf{k}\omega}^* \tag{72}$$

To calculate the distribution function versus the potential, we use a ballooning representation. The electric potential is written in the form

$$\begin{aligned} \phi(r,\theta,\varphi,t) &= \sum_{p=-\infty}^{+\infty}\tilde{\phi}_{\mathbf{k}\omega}(\theta+2p\pi,t) \\ &\quad \exp\left\{in\left[\varphi-q(r)\left(\theta+2p\pi-\theta_k\right)\right]-i\omega t\right\} \end{aligned} \tag{73}$$

where θ_k is the ballooning mode. The single term $p = 0$ is kept for strongly ballooned fluctuations. A similar expansion is used for the non adiabatic part of the distribution function, i.e. $\tilde{G}_{\mathbf{k}\omega} = \tilde{F}_{\mathbf{k}\omega} + \frac{e}{T_i}\tilde{\phi}_{\mathbf{k}\omega}$. The gyrokinetic equation Eq.(32) reads

$$(\omega - K_\parallel v_\parallel - \omega_D)\tilde{G}_{\mathbf{k}\omega} = F_M(\omega-\omega_*)\frac{e}{T_i}\left(\mathcal{J}\cdot\tilde{\phi}_{\mathbf{k}\omega}\right) \tag{74}$$

Here $K_\parallel$ is an operator

$$K_\parallel = -i\frac{1}{q_0 R_0}\frac{\partial}{\partial \eta} \tag{75}$$

where $\eta = \theta - \theta_k$ is a shifted poloidal angle. The kinetic curvature drift frequency ω_D is defined as

$$\omega_D(\eta) = \left(\frac{v_\perp^2}{2v_{Ti}^2} + \frac{v_\parallel^2}{v_{Ti}^2}\right)\omega_d(\eta) \tag{76}$$

where

$$\omega_d(\eta) = -\frac{2K_\theta T_i}{eB_0 R_0}\left[\cos\left(\theta_k + \eta\right) + s_0\eta\sin\left(\theta_k + \eta\right)\right] \tag{77}$$

$v_{Ti} = \sqrt{T_i/m_i}$ is the thermal ion velocity, and $K_\theta = \frac{-nq_0}{r_0}$ is the poloidal wavenumber - q_0 is the safety factor at the reference radius r_0. The definition of the kinetic diamagnetic frequency ω_* is the usual one

$$\omega_* = \omega_{*n} + \omega_{*T}\left(\frac{v_\perp^2}{v_{Ti}^2} + \frac{v_\parallel^2}{v_{Ti}^2} - \frac{3}{2}\right) \tag{78}$$

where

$$\begin{aligned}\omega_{*n} &= -\tfrac{K_\theta T_i}{eB_0 L_{n_i}} \\ \omega_{*T} &= -\tfrac{K_\theta T_i}{eB_0 L_{T_i}}\end{aligned} \tag{79}$$

are the density and temperature diamagnetic frequencies and L_{n_i} and L_{p_i} are the density and pressure gradient lengths calculated at the reference radius r_0. The gyroaverage $\mathcal{J}$ is fairly well represented by a Bessel function with an argument $K_\perp\rho_c$, i.e. $J_0\left(K_\perp\rho_c\right)$, where $\rho_c = \frac{m_i v_\perp}{eB_0}$ is the kinetic ion gyroradius and

$$K_\perp^2 = K_\theta^2\left[1 + s_0^2\eta^2\right] \tag{80}$$

The solution of the gyrokinetic equation Eq.(74) involves an integro-differential operator that relates $\tilde{G}_{\mathbf{k}\omega}$ to $\tilde{\phi}_{\mathbf{k}\omega}$ [34, 36]. A formal solution can be written in a Wentzel-Kramers-Brilloin (WKB) sense by dividing the r.h.s. of Eq.(74) by the resonant term $\omega - K_\parallel v_\parallel - \omega_D$

$$\tilde{F}_{\mathbf{k}\omega} = -F_M\left\{1 - \frac{\omega - \omega_*}{\omega - \omega_D - K_\parallel v_\parallel + i0^+}\right\}\frac{e\tilde{\phi}_{\mathbf{k}\omega}}{T} \tag{81}$$

We assume that the spectral turbulence intensity is of the form

$$\left|\tilde{\phi}_{\mathbf{k}\omega}\right|^2 = \mathcal{A}_{\mathbf{k}}(\theta)\left|\phi_{\mathbf{k}}\right|^2\frac{1}{\pi}\frac{\Delta\omega_{\mathbf{k}}}{(\omega - \omega_{\mathbf{k}})^2 + \Delta\omega_{\mathbf{k}}^2} \tag{82}$$

which gives

$$\left\langle \Pi^E_{r\|}(\theta,t)\right\rangle_t = \frac{1}{N}\sum_{\mathbf{k}\omega}\int d^3\mathbf{v}F_M v_\| \left|v_{E\mathbf{k}}\right|^2 \frac{eB_0}{K_\theta T_i}\left(\omega-\omega_*\right) \frac{\Delta\omega_\mathbf{k}}{(\omega-\omega_\mathbf{k})^2+\Delta\omega_\mathbf{k}^2}\delta\left(\omega-K_\| v_\| -\omega_D\right) \quad (83)$$

In the hydrodynamic limit $\frac{\omega_D}{\omega}\simeq\frac{K_\|^2 v_\|^2}{\omega^2}\ll 1$, one gets the result

$$\left\langle \Pi^E_{r\|}\right\rangle_{\theta,t} = \sum_\mathbf{k} C_{\|,\mathbf{k}0}\frac{\omega_c\Delta\omega_\mathbf{k}}{\omega_\mathbf{k}^2+\Delta\omega_\mathbf{k}^2}\left\langle\left|v_{E\mathbf{k}}\right|^2\right\rangle_t\theta_k \quad (84)$$

This result is identical to Eq.(30) with $\tau_\mathbf{k}=\frac{\Delta\omega_\mathbf{k}}{\omega_\mathbf{k}^2+\Delta\omega_\mathbf{k}^2}$. Strictly speaking there is also a contribution to the $E\times B$ flux of parallel momentum that comes from the axisymmetric perturbations of the potential $\phi_{\ell\omega}$ Eq.(43) and the distribution function response Eq.(38) . However this contribution is of second order in ballooning angle θ_k and will not be retained here. Hence the $E\times B$ flux of momentum is in this peculiar case "turbulent", i.e. produced by small scale fluctuations.

C Taylor identity

The purpose of this appendix is to demonstrate the identity

$$\frac{1}{B_0}\int_0^{2\pi}\frac{d\varphi}{2\pi}\left(\mathbf{v}_E\cdot\nabla\right)\Omega = \nabla_\perp^2\Pi^E_{r\theta} \quad (85)$$

where $\Omega=\nabla_\perp^2\phi$ is the vorticity, and $\mathbf{v}_E=\mathbf{b}\times\frac{\nabla\phi}{B}$ the $E\times B$ drift velocity. The demonstration is restricted to a geometry of concentric circular surfaces with large aspect ratio . We use the mode structure Eq.(7)

$$\phi(r,\theta,\varphi,t)=\sum_\mathbf{k}\tilde\phi_\mathbf{k}(r_0,\theta,t)\exp\left\{in\chi_\mathbf{k}\right\} \quad (86)$$

where $\chi_\mathbf{k}=\varphi-q(r)\left(\theta-\theta_k\right)$, and the dependence on r_0 is explicit for clarity throughout this section. The average over ϕ implies that the l.h. s. of Eq.(85) appears as a sum over the index $\mathbf{k}$ of operators acting on $\tilde\phi_\mathbf{k}$, namely

$$\int_0^{2\pi}\frac{d\varphi}{2\pi}\frac{\mathbf{b}}{B_0^2}\cdot\left(\nabla\phi\times\nabla\Omega\right)=\sum_\mathbf{k}\frac{\mathbf{b}}{B_0^2}\cdot\left[(\nabla\phi)_\mathbf{k}\times(\nabla\Omega)^*_\mathbf{k}\right] \quad (87)$$

where

$$(\nabla\phi)_\mathbf{k}=\frac{\partial\tilde\phi_\mathbf{k}}{\partial r_0}\nabla r_0+\frac{\partial\tilde\phi_\mathbf{k}}{\partial\theta}\nabla\theta+in\nabla\chi_\mathbf{k}\tilde\phi_\mathbf{k} \quad (88)$$

and $(\nabla\Omega)_{\mathbf{k}}$ is given by a similar expression. This suggests a change of variables for each $\mathbf{k}$, namely

$$r_0 = r \tag{89}$$

$$\chi_{\mathbf{k}} = \varphi - q(r)\,(\theta - \theta_k) \tag{90}$$

$$\eta = \theta \tag{91}$$

The variable η plays the role of a coordinate along the field line, r_0 represents the slow variation of the field in the radial electric field, and $\chi_{\mathbf{k}}$ is a coordinate transverse to the field. We use the following ordering

$$\frac{1}{R_0}\frac{\partial\tilde{\phi}_{\mathbf{k}}}{\partial\eta} \ll \frac{\partial\tilde{\phi}_{\mathbf{k}}}{\partial r_0} \ll \frac{nq_0}{r_0}\tilde{\phi}_{\mathbf{k}} \tag{92}$$

which allows neglecting the slow variation of the field along the field line. We note that the unit vector along the magnetic field can be written,

$$\mathbf{b} = \frac{r_0}{q_0}\nabla\chi_{\mathbf{k}} \times \nabla r_0 \tag{93}$$

for any $\mathbf{k}$. Ignoring the derivatives with respect to η, one finds the following identity

$$\int_0^{2\pi} \frac{d\varphi}{2\pi}\frac{\mathbf{b}}{B_0^2}\cdot(\nabla\phi\times\nabla\Omega) = \frac{1}{B_0^2}\frac{q_0}{r_0}\frac{\partial}{\partial r_0}\left\{\sum_{\mathbf{k}}\left(in\tilde{\phi}_{\mathbf{k}}\Omega^*_{\mathbf{k}}\right)\right\} \tag{94}$$

where $|\nabla\chi_{\mathbf{k}}|^2 \simeq \frac{q_0^2}{r_0}$ for a ballooned turbulence. Using $\nabla_\perp^2 = \nabla\cdot\nabla - (\mathbf{b}\cdot\nabla)^2$, and neglecting again the derivatives along the field lines. Each Fourier harmonics of the vorticity can be written as

$$\Omega_{\mathbf{k}} = \frac{1}{r_0}\frac{\partial}{\partial r_0}r_0\frac{\partial}{\partial r_0}\left(r_0\tilde{\phi}_{\mathbf{k}}\right) + 2in\,(\nabla\chi_{\mathbf{k}}\cdot\nabla r_0)\,\frac{\partial}{\partial r_0}\tilde{\phi}_{\mathbf{k}} - n^2\,|\nabla\chi_{\mathbf{k}}|^2\,\tilde{\phi}_{\mathbf{k}} \tag{95}$$

where it has been used that the variation of $\tilde{\phi}_{\mathbf{k}}$ with r_0 is faster than the radial variation of $(\nabla\chi_{\mathbf{k}}\cdot\nabla r_0)$. The largest term is the third one in the r.h.s. of Eq.(95) , but it does not contribute to Eq.(94) for parity reasons. The largest contribution therefore comes from the second term of the r.h.s. of Eq.(95) , i.e.

$$\int_0^{2\pi} \frac{d\varphi}{2\pi}\frac{\mathbf{b}}{B_0^2}\cdot(\nabla\phi\times\nabla\Omega) \simeq \nabla_\perp^2\left[-\sum_{\mathbf{k}} s_0(\eta-\theta_k)\left|\frac{nq_0}{r_0}\frac{\tilde{\phi}_{\mathbf{k}}}{B_0}\right|^2\right] \tag{96}$$

where

$$\nabla_\perp^2 = \frac{1}{r_0}\frac{\partial}{\partial r_0}r_0\frac{\partial}{\partial r_0} \tag{97}$$

The expression within the brackets of the r.h.s. of Eq.(96) is the $r\theta$ component of the $E\times B$ stress tensor, as can be verified from Eq.(21). Eq.(96) demonstrates the Taylor identity Eq.(85).

D Linear calculation of radial and parallel wavenumber

Assuming an electron adiabatic response, and using the solution of the gyro-kinetic equation Eq.(81), the following electroneutrality equation is obtained for a non axisymmetric mode $n \neq 0$

$$\left\{\tau + 1 - \frac{1}{N}\int d^3\mathbf{v} F_M \mathcal{J} \frac{\omega - \omega_*}{\omega - K_\parallel v_\parallel - \omega_D}\mathcal{J}\right\}\tilde{\phi}_{\mathbf{k}\omega} = 0 \qquad (98)$$

where $\tau = \frac{T_i}{T_e}$ is the ratio of the ion to electron temperature at $r = r_0$. This equation, which describes reasonably well toroidal ITG modes, can be easily extended to non adiabatic electrons [34](see also [35] and references therein). In the hydrodynamic limit

$$\frac{\omega_D}{\omega} \sim \frac{K_\parallel^2 v_{Ti}^2}{\omega^2} \sim K_\perp^2 \rho_i^2 \ll 1 \qquad (99)$$

the electro-neutrality condition Eq.(98) can be expanded at first order in $\frac{\omega_D}{\omega}$, $\frac{K_\parallel^2 v_{Ti}^2}{\omega^2}$ and $K_\perp^2\rho_i^2$, where $\rho_i = \frac{m_i v_{Ti}}{eB_0}$ is the thermal ion gyroradius. The equation that rules $\tilde{\phi}_{\mathbf{k}\omega}$ now reads [36]

$$\left[-\frac{\omega_t^2}{\omega^2}\frac{\partial^2}{\partial\eta^2} - K_\theta^2\rho_i^2(1 + s_0^2\eta^2) + \Lambda(\omega,\eta)\right]\tilde{\phi}_{\mathbf{k}\omega} = 0 \qquad (100)$$

where

$$\Lambda(\omega,\eta) = \frac{\tau\omega + \omega_{*n}}{\omega_{*p} - \omega} + \frac{\omega_d(\eta)}{\omega} \qquad (101)$$

is the η dependent local dispersion relation. The transit frequency is defined $\omega_t = \left|\frac{v_{Ti}}{q_0 R_0}\right|$ and ω_{*p} is the pressure diamagnetic frequency

$$\omega_{*p} = -\frac{K_\theta T_i}{eB_0 L_{p_i}} \qquad (102)$$

where L_{p_i} is the pressure gradient length. The next step consists in expanding the curvature drift frequency near $\eta = 0$ up to $o(\eta^2)$ and $o(\theta_k^2)$. After regrouping the various terms, one finds

$$\left[-\frac{\omega_t^2}{\omega^2}\frac{\partial^2}{\partial\eta^2} + \left(\frac{\omega_d}{\omega}\left(s_0 - \frac{1}{2}\right) - K_\theta^2\rho_i^2 s_0^2\right)(\eta - \eta_{\mathbf{k}})^2 + \Lambda\right]\tilde{\phi}_{\mathbf{k}\omega} = 0 \qquad (103)$$

where Λ is now a local dispersion relation independent of η and

$$\Lambda(\omega) = \frac{\tau\omega + \omega_{*n}}{\omega_{*p} - \omega} + \frac{\omega_d}{\omega} - K_\theta^2\rho_i^2 - \frac{1}{4}\frac{\omega_d^2}{\omega^2}\frac{(s_0 - 1)^2}{\left[\frac{\omega_d}{\omega}\left(s_0 - \frac{1}{2}\right) - K_\theta^2\rho_i^2 s_0^2\right]}\theta_k^2 \qquad (104)$$

where ω_d is the local curvature drift frequency. Strictly speaking $\omega_d = -2\frac{K_\theta T}{eB_0R_0}\left(1-\theta_k^2\right)$, but the analysis is restricted here to low values of θ_k. Calculations are run at first order in θ_k, so that the curvature drift is the one defined in Eq.(58). The complex number $\eta_{\mathbf{k}}$ is proportional to the ballooning angle θ_k

$$\eta_{\mathbf{k}} = -\frac{1}{2}\frac{\omega_d}{\omega}\frac{(s_0-1)}{\left[\frac{\omega_d}{\omega}\left(s_0-\frac{1}{2}\right)-K_\theta^2\rho_i^2 s_0^2\right]}\theta_k \tag{105}$$

The smoothest solution of this differential equation is

$$\tilde{\phi}_{\mathbf{k}\omega} = \phi_0 \exp\left\{-\frac{1}{2}\alpha_{\mathbf{k}}\left(\eta-\eta_{\mathbf{k}}\right)^2\right\} \tag{106}$$

with the conditions

$$\frac{\omega_t^2}{\varpi_{\mathbf{k}}^2}\alpha_{\mathbf{k}}^2 = \frac{\omega_d}{\varpi_{\mathbf{k}}}\left(s_0-\frac{1}{2}\right)-K_\theta^2\rho_i^2 s_0^2 \tag{107}$$

$$\frac{\omega_t^2}{\varpi_{\mathbf{k}}^2}\alpha_{\mathbf{k}} = -\Lambda(\varpi_{\mathbf{k}}) \tag{108}$$

The two equations Eqs.(107, 108) provide the values of $\alpha_{\mathbf{k}}$ and of the complex mode frequency $\varpi_{\mathbf{k}}$. Moreover, the solution Eq.(106) is acceptable only if $\Re\left(\alpha_{\mathbf{k}}\right) > 0$, to guarantee mode spatial localization. The mode frequency $\varpi_{\mathbf{k}}$ is written as $\varpi_{\mathbf{k}} = \omega_{\mathbf{k}} + i\gamma_{\mathbf{k}}$, where $\omega_{\mathbf{k}}$ is the real part, and $\gamma_{\mathbf{k}}$ the growth rate. The later is positive above the instability threshold. We will focus on that case. A limit of interest is $K_\theta\rho_i \ll 1$, and $\frac{\omega_t^2}{\omega^2}\alpha_{\mathbf{k}} \ll \Lambda$. The dispersion relation then becomes $\Lambda(\varpi_{\mathbf{k}}) = 0$, i.e.

$$\tau\varpi_{\mathbf{k}}^2 - (\omega_d-\omega_{*n})\varpi_{\mathbf{k}} + \omega_{*p}\omega_d = 0 \tag{109}$$

which yields

$$\omega_{\mathbf{k}} = \frac{1}{2\tau}(\omega_d-\omega_{*n}) \tag{110}$$

$$\gamma_{\mathbf{k}} = \frac{1}{2\tau}\left[4\tau\omega_{*p}\omega_d-(\omega_d-\omega_{*n})^2\right]^{1/2} \tag{111}$$

It is recovered that modes drift linearly in the ion diamagnetic direction for flat density profiles $\omega_{*n} \simeq 0$, while they rotate in the electron diamagnetic direction for strong density gradients [36]. We now turn to the quantities of interest, i.e. the radial and parallel wavenumber given by Eq.(14,15). Since Eq.(108) depends on the detail of the local dispersion relation, we will use exclusively Eqs.(107) and leave

$\varpi_{\mathbf{k}}$ arbitrary, except at the very end, when making estimates for ITG modes. It appears that $\delta_{\mathbf{k}} = \lambda_{\mathbf{k}} - 1$ is given by the following relation

$$\delta_{\mathbf{k}} = -\frac{\frac{\omega_d}{2\varpi_{\mathbf{k}}}(s_0 - 1)}{\frac{\omega_d}{\varpi_{\mathbf{k}}}\left(s_0 - \frac{1}{2}\right) - K_\theta^2 \rho_i^2 s_0^2} = -\frac{1}{2}\frac{\omega_d \varpi_{\mathbf{k}}}{\omega_t^2}\frac{1}{\alpha_{\mathbf{k}}^2}(s_0 - 1) \tag{112}$$

from which its imaginary part $\Im\left(\delta_{\mathbf{k}}\right)$ can be deduced

$$\Im\left(\delta_{\mathbf{k}}\right) = -\frac{1}{2}\frac{K_\theta^2 \rho_i^2 s_0^2 (s_0 - 1)}{\left|\frac{\omega_d}{\varpi_{\mathbf{k}}}\left(s_0 - \frac{1}{2}\right) - K_\theta^2 \rho_i^2 s_0^2\right|^2}\frac{\gamma_{\mathbf{k}}\omega_d}{\left|\varpi_{\mathbf{k}}\right|^2} \tag{113}$$

thus leading to

$$K_{\parallel,0} = -\frac{1}{2q_0 R_0} K_\theta^2 \rho_i^2 s_0^2 (s_0 - 1)\frac{1}{\Re\left(\alpha_{\mathbf{k}}\right)}\left|\frac{\varpi_{\mathbf{k}}}{\alpha_{\mathbf{k}}\omega_t}\right|^2 \frac{\gamma_{\mathbf{k}}\omega_d}{\omega_t^2}\theta_k \tag{114}$$

Using the relation $\omega_d = -2\left|q_0\right| K_\theta \rho_i \omega_t$, one gets the expression of $C_{\parallel,\mathbf{k}0}$

$$C_{\parallel,\mathbf{k}0} = \mathrm{sgn}(q_0)\frac{\rho_i}{R_0}\left(K_\theta \rho_i s_0\right)^2 (s_0 - 1)\frac{1}{\Re\left(\alpha_{\mathbf{k}}\right)}\left|\frac{\varpi_{\mathbf{k}}}{\alpha_{\mathbf{k}}\omega_t}\right|^2 \frac{\gamma_{\mathbf{k}}}{\omega_t} \tag{115}$$

The calculation of $K_{r,0}$ is somewhat more delicate because of compensation effects. Using the r.h.s of Eq.(112), one finds

$$C_{r,\mathbf{k}0} = \frac{K_{r,0}}{K_\theta \theta_k} = -\frac{1}{2}\frac{\omega_d}{\omega_t^2} s_0 \left(s_0 - 1\right)\frac{\Re\left(\frac{\varpi_{\mathbf{k}}}{\alpha_{\mathbf{k}}}\right)}{\Re\left(\alpha_{\mathbf{k}}\right)} \tag{116}$$

It appears readily that

$$C_{r,\mathbf{k}0} = -\frac{1}{2} s_0 \left(s_0 - 1\right)\frac{\omega_d \omega_{\mathbf{k}}}{\omega_t^2}\frac{\sigma_{\mathbf{k}}}{\left|\alpha_{\mathbf{k}}\right|^2} \tag{117}$$

where

$$\sigma_{\mathbf{k}} = 1 - \frac{\Im\left(\alpha_{\mathbf{k}}\right)}{\Re\left(\alpha_{\mathbf{k}}\right)}\frac{\gamma_{\mathbf{k}}}{\omega_{\mathbf{k}}} \tag{118}$$

The condition Eq.(107) can be used to provide a relation between $\Re\left(\alpha_{\mathbf{k}}\right)$ and $\Im\left(\alpha_{\mathbf{k}}\right)$, i.e.

$$2\Re\left(\alpha_{\mathbf{k}}\right)\Im\left(\alpha_{\mathbf{k}}\right) = \frac{\gamma_{\mathbf{k}}\omega_{\mathbf{k}}}{\omega_t^2}\left[\frac{\omega_d}{\omega_{\mathbf{k}}}\left(s_0 - \frac{1}{2}\right) - 2K_\theta^2 \rho_i^2 s_0^2\right] \tag{119}$$

from which one gets the following result

$$\sigma_{\mathbf{k}} = 1 - \left[\frac{\omega_d}{2\omega_{\mathbf{k}}}\left(s_0 - \frac{1}{2}\right) - K_\theta^2 \rho_i^2 s_0^2\right]\frac{\gamma_{\mathbf{k}}^2}{\left[\Re\left(\alpha_{\mathbf{k}}\right)\right]^2 \omega_t^2} \tag{120}$$

An explicit expression of $[\Re(\alpha_{\mathbf{k}})]^2$ can be found by solving Eq.(107) , i.e.

$$\begin{aligned}[\Re(\alpha_{\mathbf{k}})]^2 &= \frac{1}{2\omega_t^2}\left[\omega_{\mathbf{k}}\omega_d\left(s_0-\frac{1}{2}\right)-K_\theta^2\rho_i^2 s_0^2\left\{\omega_{\mathbf{k}}^2-\gamma_{\mathbf{k}}^2\right\}\right] \\ &+ \frac{1}{2\omega_t^2}\left\{\left[\omega_{\mathbf{k}}\omega_d\left(s_0-\frac{1}{2}\right)-K_\theta^2\rho_i^2 s_0^2\left\{\omega_{\mathbf{k}}^2-\gamma_{\mathbf{k}}^2\right\}\right]^2\right. \\ &+ \left.\gamma_{\mathbf{k}}^2\left[\omega_d\left(s_0-\frac{1}{2}\right)-2K_\theta^2\rho_i^2 s_0^2\omega_{\mathbf{k}}\right]^2\right\}^{1/2} \qquad (121)\end{aligned}$$

It results from Eq.(120) that $C_{r,\mathbf{k}0}$ changes sign when

$$\frac{\gamma_{\mathbf{k}}^2}{[\Re(\alpha_{\mathbf{k}})]^2\omega_t^2} \geq \frac{1}{\frac{\omega_d}{2\omega_{\mathbf{k}}}\left(s_0-\frac{1}{2}\right)-K_\theta^2\rho_i^2 s_0^2} \qquad (122)$$

provided the r.h.s. is positive. The positivity condition is fulfilled for modes drifting in the ion diamagnetic direction $\mathrm{sgn}(\omega_d\omega_{\mathbf{k}})$ for low wave numbers and positive magnetic shear. This change of sign typically occurs when one moves from the situation of weak drive (near threshold) $\gamma_{\mathbf{k}} \ll \omega_{\mathbf{k}}$ to a situation of strong drive $\gamma_{\mathbf{k}} \gg \omega_{\mathbf{k}}$.

To make these expressions more explicit, we concentrate on the limit of a strong magnetic shear $|s_0| >> 1$ and low wavenumbers $K_\theta^2\rho_i^2 \ll 1$. Using the relations Eq.(119, 121), explicit expressions of $\Re(\alpha_{\mathbf{k}})$, $\Im(\alpha_{\mathbf{k}})$ can be found

$$[\Re(\alpha_{\mathbf{k}})]^2 = \frac{1}{2}\frac{|\omega_{\mathbf{k}}\omega_d s_0|}{\omega_t^2}\lambda_+ \qquad (123)$$

$$[\Im(\alpha_{\mathbf{k}})]^2 = \frac{1}{2}\frac{|\omega_{\mathbf{k}}\omega_d s_0|}{\omega_t^2}\lambda_- \qquad (124)$$

from which $\sigma_{\mathbf{k}}$ and $|\alpha_{\mathbf{k}}|^2$ can be derived

$$\sigma_{\mathbf{k}} = 1 - \mathrm{sgn}(\omega_{\mathbf{k}}\omega_d s_0)\lambda_- \qquad (125)$$

$$|\alpha_{\mathbf{k}}|^2 = \frac{|\omega_{\mathbf{k}}\omega_d s_0|}{\omega_t^2}\left(1+\frac{\gamma_{\mathbf{k}}^2}{\omega_{\mathbf{k}}^2}\right)^{1/2} \qquad (126)$$

where

$$\lambda_\pm = \left[\left(1+\frac{\gamma_{\mathbf{k}}^2}{\omega_{\mathbf{k}}^2}\right)^{1/2} \pm \mathrm{sgn}(\omega_{\mathbf{k}}\omega_d s_0)\right] \qquad (127)$$

The numbers λ_+ and λ_- are always positive, and satisfy the useful relationships

$$\lambda_+\lambda_- = \frac{\gamma_{\mathbf{k}}^2}{\omega_{\mathbf{k}}^2} \qquad (128)$$

$$\lambda_+ + \lambda_- = 2\left(1 + \frac{\gamma_{\mathbf{k}}^2}{\omega_{\mathbf{k}}^2}\right) \tag{129}$$

The expression Eq.(126) of $|\alpha_{\mathbf{k}}|^2$ can be obtained directly from Eq.(107), thus providing a cross-check . Plugging Eqs.(128,129) in the expressions of $C_{\parallel,\mathbf{k}0}$ and $C_{r,\mathbf{k}0}$ Eqs.(114,117), one obtains the following relations

$$C_{r,\mathbf{k}0} = c_{r\mathbf{k}} s_0 \tag{130}$$

$$C_{\parallel,\mathbf{k}0} = c_{\parallel\mathbf{k}} \frac{\rho_i}{R_0} \left(K_\theta \rho_i s_0\right)^2 q_0 s_0 \tag{131}$$

where $c_{r\mathbf{k}}$ and $c_{\parallel\mathbf{k}}$ are numbers that depend on the normalized frequencies $\frac{\omega_{\mathbf{k}}}{\omega_d}$ and $\frac{\gamma_{\mathbf{k}}}{\omega_d}$ only, namely

$$c_{r\mathbf{k}} = \frac{1}{2} \frac{1}{\left(1 + \frac{\gamma_{\mathbf{k}}^2}{\omega_{\mathbf{k}}^2}\right)^{1/2}} \left(\lambda_- - \mathrm{sgn}\left(\omega_{\mathbf{k}} \omega_d s_0\right)\right) \tag{132}$$

$$c_{\parallel\mathbf{k}} = 2^{1/2} \frac{1}{|q_0|} \left|\frac{\omega_{\mathbf{k}}}{\omega_d s_0}\right|^{3/2} \left(1 + \frac{\gamma_{\mathbf{k}}^2}{\omega_{\mathbf{k}}^2}\right)^{1/2} \lambda_-^{1/2} \tag{133}$$

References

[1] T. Vernay, S. Brunner, L. Villard et al., Physics of Plasmas **19**, 042301 (2012).

[2] M. Oberparleiter, Ph.D. thesis, Universität Ulm (2015); M. Oberparleiter, F. Jenko, D. Told, H. Doerk, T. Görler, submitted to Phys. Plasmas (2015).

[3] G. Dif-Pradalier, V. Grandgirard, Y. Sarazin et al., Phys. Rev. Lett. **103**, 065002 (2009).

[4] F.I. Parra and P.J. Catto, Plasma Phys. Control. Fusion **52**, 059801 (2010).

[5] M. Barnes, F. I. Parra, J. P. Lee et al., Phys. Rev. Letters **111**, 055005 (2013).

[6] J. Abiteboul, X. Garbet, V. Grandgirard, S. J. Allfrey, Ph. Ghendrih, G. Latu, Y. Sarazin, and A. Strugarek, Phys. Plasmas **18**, 082503 (2011).

[7] Y. Idomura Phys. Plasmas **21**, 022517 (2014).

[8] J.W. Connor, R.J. Hastie and J.B. Taylor, Proc. R. Soc. London Ser. A **365**, 1 (1979).

[9] F. Romanelli and F. Zonca, Phys. Fluids B 5, 4081 (1993).

[10] J. W. Connor, J. B. Taylor, and H. R. Wilson, Phys. Rev. Letters **70**, 1803 (1993).

[11] J.Y. Kim and M. Wakatani, Phys. Rev. Letters **73**, 2200 (1994).

[12] R. E. Waltz, R. L. Dewar, and X. Garbet, Physics of Plasmas **5**, 1784 (1998).

[13] Y. Kishimoto, J.-Y. Kim, W. Horton, T. Tajima, M. J. LeBrun, and H. Shirai, Plasma Phys. Controlled Fusion **41**, A663 (1999).

[14] C. J. McDevitt, Xian-Zhu Tang, and Zehua Guo, Phys. Rev. Letters **111**, 205002 (2013).

[15] D. Estève, Y. Sarazin, X. Garbet, et al. submitted to Nuclear Fusion.

[16] P. W. Terry, Reviews of Modern Physics **72**, 109 (2000).

[17] Y. Camenen, Y. Idomura, S. Jolliet and A.G. Peeters Nucl. Fusion **51**, 073039 (2011) .

[18] P. H. Diamond, C. J. McDevitt, Ö. D. Gürcan, T. S. Hahm and V. Naulin, Phys. Plasmas **15**, 012303 (2008).

[19] R.R. Dominguez and G.M. Staebler Phys. Fluids B **5**, 3876 (1993).

[20] Diamond P.H. *et al* 1994 in Plasma Physics and Controlled Nuclear Fusion Research 1994 (Proc. 15th Int. Conf. Seville, 1994), Vol. 3, p. 323, IAEA, Vienna (1995)

[21] X. Garbet , Y. Sarazin, Ph. Ghendrih *et al* Phys. Plasmas **9**, 3893 (2002).

[22] P.H. Diamond, C.J. McDevitt, Ö .D. Gürcan, et al., Nucl. Fusion **49**, 045002 (2009).

[23] A.G. Peeters, C. Angioni, A. Bortolon, et al., Nucl. Fusion **51**, 094027 (2011).

[24] M. McIntyre, "On Global-Scale Atmospheric Circulations", in "Perspective in Fluid Dynamics", Cambridge University Press, eidted by G.K. Batchelor, H.K. Moffatt, and H.K. Worster, p. 610 (2000).

[25] P. H. Diamond, Y.-M. Liang, B. A. Carreras, and P. W. Terry Phys. Rev. Lett. **72**, 2565 (1994).

[26] P. H. Diamond, S-I. Itoh, K. Itoh and T. S. Hahm, Plasma Phys. Control. Fusion **47**, 35 (2005) .

[27] M.N. Rosenbluth, P.H. Rutherford, J.P. Taylor, E.A. Frieman, and L.M. Kovrizhnykh, Plasma Physics and Controlled Nuclear Fusion Research IAEA, Vienna, 1971, Vol. 1, p. 495.

[28] S. K Wong. and V. S. Chan , Physics of Plasmas **14**, 112505 (2007)

[29] S. K Wong. and V. S. Chan , Physics of Plasmas **16**, 122507 (2009).

[30] A. Smolyakov,"Elements of Neoclassical Theory of Plasma Rotation in a Tokama", in Review of the Theory of Magnetized Plasmas,"Rotation and Momentum Transport in Magnetized Plasma", World Scientific, Vol II, p.173 (2015).

[31] V. Grandgirard, J. Abiteboul, J. Bigot et al., Computer Physics Communications **207**, 35 (2016).

[32] R. J. Fonck, G. Cosby, R. D. Durst, et al. Phys. Rev. Lett. **70**, 3736 (1993).

[33] P. Hennequin, R. Sabot, C. Honoré et al. Plasma Phys. Control. Fusion **46**, B121 (2004).

[34] G. Rewoldt, W. M. Tang, and M. S. Chance, Physics of Fluids **25**, 480 (1982).

[35] W. Horton, Reviews of Modern Physics **71**, 735 (1999).

[36] F. Romanelli, Physics of Fluids B **1**, 1018 (1989).